

Phase-Averaged Measurements of Unsteady Flow in a Vaneless Diffuser

R. M. C. So,* M. V. Otugen,† F. Baban‡
Arizona State University, Tempe, Arizona 85287
 and

B. C. Hwang§
Naval Ship Research and Development Center, Annapolis, Maryland 21402

The unsteady, periodic flow inside a vaneless diffuser was investigated experimentally. Flow through the model diffuser was delivered by an actual impeller and exited to room conditions. The mass flow rate through the diffuser was chosen to be high enough so that an unstalled diffuser flow was obtained in spite of the presence of a shroud-side recirculation ring. A phase-locked ensemble-averaging technique was used to resolve the unsteady, periodic velocities inside the diffuser. This was accomplished by monitoring the radial velocity at the diffuser inlet using a single hot wire, thus providing the required reference phase of the diffuser flow. The flowfield was measured using a cross wire and the ensemble-averaged, time-resolved distributions of flow angle, radial and circumferential velocities, and their respective statistics were calculated and reported. The recirculating flow was measured using a one-component laser Doppler velocimeter. These results indicate that the recirculation ring starts just downstream of the diffuser inlet and covers about 80% of the diffuser in the radial direction. At its maximum, the axial extent of the recirculation ring is about 35% of the diffuser width. Furthermore, the radial decay of the circumferentially asymmetric character of the flow is relatively slow, and the periodic behavior persists even at the diffuser exit. Finally, the measurements serve as a valuable data set for the validation of diffuser calculation models.

Nomenclature

b	= diffuser width, = 2.54 cm
h	= impeller channel height at the exit, = 1.88 cm
p_w	= wall static pressure
p_0	= atmospheric pressure
ΔP	= pressure difference, = $p_w - p_0$
\bar{r}	= normalized radial coordinate, = $(r - r_i)/(r_o - r_i)$
r	= dimensional radial coordinate
U_{TIP}	= impeller tip speed
v_r, v'_r	= fluctuating radial velocity and its rms, respectively
V_r, V_z	= mean radial and axial velocity, respectively
v_θ	= fluctuating circumferential velocity
v'_θ	= rms of fluctuating circumferential velocity
V_θ	= mean circumferential velocity
z	= axial coordinate measured from diffuser hub
α	= mean flow angle measured from the circumferential coordinate
θ	= circumferential coordinate
ρ	= fluid density
Ω	= rotational speed of impeller

Introduction

THE flow entering a vaneless diffuser is circumferentially and axially asymmetric because of the passage of the impeller blades and the nonuniform flow distribution across each impeller channel. This circumferential nonuniformity can be quite pronounced, depending on the impeller design, the rota-

tional speed, and the operating mass flow rate. The extent of these asymmetries and their rate of decay with radial distance inside the vaneless diffuser can significantly affect the overall efficiency of radial compressors and the noise generated by them. In order to develop a reliable diffuser model, whereby all these characteristics can be calculated, a thorough understanding of diffuser flow is required.

Unfortunately, very few detailed experimental investigations of vaneless diffuser flow are available. This is due partly to the complexity of the flow and partly to difficulty in successfully employing conventional measurement techniques to measure the mean and fluctuating flow properties. These difficulties kept many researchers from tackling the problem. An early attempt was made by Dean and Senoo,¹ who measured the mean radial velocity and the flow angle in a vaneless diffuser to support their theoretical predictions. The experiment was crude; conventional time-averaging was used to obtain the mean velocity, and a field of tufts was used to determine the mean flow angle. More advanced measurement techniques, such as high-response, shielded hot wires,² hot-wire anemometry,³ and laser velocimetry⁴ were later used to study the velocity field inside radial compressors. Unfortunately, measurements concerning the vaneless diffuser section were limited to the inlet of the diffuser in all these studies. Furthermore, with the exception of Ref. 4, the mean flow properties were obtained by time-averaging the nonconditionally sampled data records, thereby lumping together the jet and the wake regions. Here, the term "jet" is used to refer to the flow coming out of the passage between the blades, and "wake" refers to the flow directly behind the blade. It is usual practice to consider the flow bounded by the central planes of adjacent passages and refer to it as a jet/wake type of flow. Nevertheless, the time progress of the instantaneous radial velocity confirms the strong circumferential nonuniformity of the flow conditions at the diffuser inlet.⁴ These results also indicate an axial distribution of the mean radial velocity that is strongly skewed. Although not extensive, the above studies put in plain view the complexity of the conditions at the diffuser inlet.

Received Jan. 13, 1989; revision received Aug. 15, 1989. Copyright © 1989 by R. So. Published by the American Institute of Aeronautics and Astronautics, Inc. All rights reserved.

*Professor, Mechanical and Aerospace Engineering.

†Assistant Professor, Aerospace Engineering, Polytechnic University, Farmingdale.

‡Graduate Assistant, Mechanical and Aerospace Engineering.

§Research Scientist.

At the exit of an impeller, the velocity distribution across each channel is often nonuniform in both the axial and circumferential directions, in addition to the wake created by the passage of the impeller blades. Usually, the growth of the boundary layer along one side of the impeller blade is larger than it is on the opposite side. This is due to pressure gradients caused by the rotation of the impeller and, in the case of cambered impellers, is due also to the sharp bend in the flow channel. Therefore, inlet conditions to vaneless diffusers can vary widely depending on the impeller providing the flow. Senoo and Ishida⁵ specifically addressed the periodic, jet/wake type of behavior of the flow by creating a severely asymmetric flow at the inlet to the diffuser, using a model impeller, and monitored its decay radially. They recorded the time progress of the velocity signal at various locations inside the vaneless diffuser. The jet/wake type of flow was preserved at radial distance far away from the diffuser inlet. This was evident in the steep circumferential gradients of the velocity obtained at locations where the velocity difference between the jet and the wake regions had become small. The study suggested that the flow was unsteady and circumferentially nonuniform, not just at the inlet but also at large radial distance away from the inlet. This ran contrary to the earlier belief that the strong circumferential mixing would cause the flow to become uniform soon after it entered the diffuser.

There is evidence that the unsteady, jet/wake-type inlet conditions are preserved at large radial distance in vaneless diffusers. This point needs to be further investigated experimentally, especially in diffusers coupled with actual impellers, which produce realistic inlet conditions. In fact, if any portion of the diffuser flow is indeed circumferentially and axially nonuniform, then detailed numerical analysis of this flow will require a complete specification of all inlet conditions. Therefore, diffuser measurements, if they are to serve as data for model validation, should strive to provide complete information at the inlet. In light of the fact that such a set of data is not available, the present objective is to attempt to measure the stall-free flow in a vaneless diffuser so that the measurements can be used to validate diffuser calculation models.

The measurement and analysis techniques used in previous investigations cannot be relied on to produce detailed information on the flowfield. First of all, time-series data records

of velocity, without the use of a proper time-averaging method, cannot reveal the statistical behavior of the mean and turbulent flow. On the other hand, straightforward time-averaging of the nonconditionally sampled time records of velocity, measured at a single flow location, will ignore the nonstationary and nonuniform behavior of the velocity. Flow statistics obtained in this fashion will lump together the characteristics of the jet/wake type of flows and probably cannot provide useful information for the development of a realistic vaneless diffuser flow model.

In the present investigation, a phase-locked sampling technique was used to overcome the above-mentioned difficulties. At any given time, the nonuniform velocity distribution has a pattern that repeats itself around the periphery of the diffuser and is synchronous with the impeller channels. Similarly, at a fixed circumferential location, the same pattern can be observed and is periodic in time as the impeller channels go past this location. Hence, the circumferentially periodic distribution of the flow properties was measured using a cross-wire probe fixed at one circumferential location inside the diffuser. In order to isolate the periodic behavior of the mean flow properties in each data record, time-averaging was performed on the data having the same phase angle. The correct phase angle was determined from a reference hot wire placed at the diffuser inlet. Thus sampled, the data could be analyzed to give the period-resolved statistical properties, such as the mean flow angle, mean velocities, and turbulent stresses. This technique is similar to the one used by Cenedese et al.⁶ to study the turbulent wake behavior behind a propeller.

Test Rig and Instrumentation

Experiments were carried out in the model compressor system of Otugen et al.⁷ The test rig consisted of an intake channel, an actual impeller, and a vaneless diffuser. The flow entered the intake channel through a streamlined opening with an adjustable plug to control the mass flow rate. However, the present experiments were conducted at a fixed mass flow rate of 0.162 kg/s, which was high enough to insure a stall-free flow in the diffuser. The flow exited into room conditions and, thus the pressure distribution at the diffuser exit was circumferentially uniform.

An actual compressor impeller (Model T-67), provided by the Naval Ship Research and Development Center of the U.S. Navy, was used to deliver the flow to the vaneless diffuser (Fig. 1). The impeller has 17 blades. At the inlet of the impeller, there were no splitter plates, and the blades were aligned in the radial direction. At the exit, the channel height was 1.88 cm, and the blades were backswept with an angle of 45 deg. Thus, the impeller channels were strongly cambered. The impeller inlet diameter was 18.42 cm, whereas it measured 35.56 cm at the outlet. The diffuser had parallel walls with a width of $b = 2.54$ cm, and the diffuser outlet-to-inlet radius ratio was 1.5. The impeller was driven by a 7.5-hp electric motor at a rotational speed of $\Omega = 924$ rpm. This produced a Reynolds number of about 25,900, based on the impeller tip speed and the diffuser width.

Hot-wire anemometry was used to measure the velocity field. A cross-wire miniature probe (DISA Model 55P61), whose sensor plane was parallel to the diffuser walls, was used to traverse the vaneless diffuser both in the axial z and the radial r directions at a fixed circumferential position. In this way, the instantaneous radial and circumferential velocities were recorded at various locations in the diffuser. The cross-wire probe was inserted into the flow from the diffuser exit so that the probe support and its axis were parallel to the radial direction. This mode of probe insertion was preferred because it offered minimum disturbance to the jet/wake type of flow at the measuring location. In addition to the cross wire, a straight-wire probe (DISA, Model 55P11), introduced through the shroud wall, was used to measure the radial velocity at the diffuser inlet. Its purpose was to provide a reference signal, which was necessary for the phase-locked analysis. It was

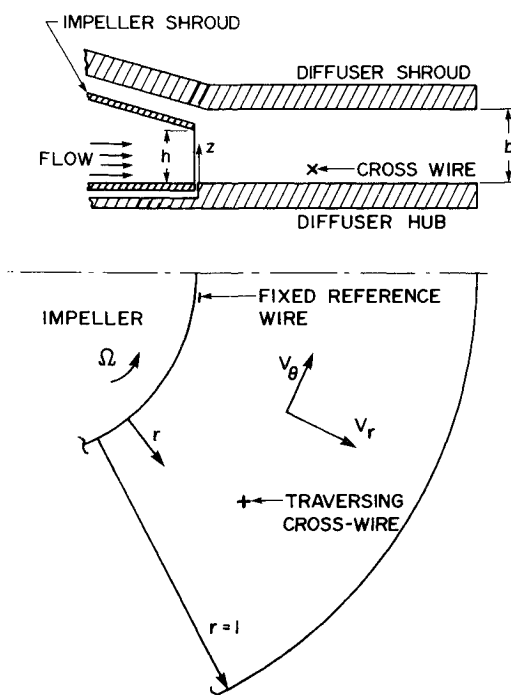


Fig. 1 Schematic of diffuser test section.

placed at a normal position of $z/b=0.36$. The straight-wire probe was not placed along the same radial line as the cross-wire probe. Instead, it was located at a different circumferential location (Fig. 1). Since the start of a period at any flow location was judged by this reference radial velocity, the precise location of this straight wire was kept intact throughout the experiment.

Both the cross-wire and the straight-wire probes were used in conjunction with DISA Model 56C01 constant-temperature anemometers (CTA), which were equipped with Model 56C10 bridges and Model 56N21 linearizers. The frequency response of the hot-wire instrumentation was set at 40 kHz, which was high enough to resolve the periodic behavior of the diffuser flow. The output from the linearizers were low-pass filtered at a frequency of 40 kHz to remove the high-frequency noise from the signals. An 8-channel, 12-bit A/D converter (Metabyte Dash 16) was used to digitize the signals, which were then recorded and analyzed on a Zenith 158 personal computer.

The onset of rotating diffuser stall has been found to be preceded by local separation on diffuser walls.^{7,8} In order to insure that an unstalled flow was indeed created for the present study, possible local flow separation had to be detected using a laser Doppler velocimeter (LDV) because conventional hot-wire anemometers cannot resolve flow direction. The laser system used in the experiments of So et al.⁹ was applied to traverse the near-wall flow and to detect flow reversal near the wall. Water/glycerin droplets (nominal diameter of 1μ), generated by a DISA 55L18 seeding generator, were used to seed the flow. The particles were introduced at the entrance of the intake channel. A 4 W argon-ion laser replaced the helium-neon laser of Ref. 10 in the hope of achieving a higher signal-to-noise ratio and thereby improving the accuracy of the measurements. In order to resolve the jet/wake behavior in the flow correctly, a sampling rate of ~ 20 kHz is required. Using the present facility and seeding technique, numerous attempts were made to sample the Doppler signal at 20 kHz. However, it was found that the highest sampling rate at which accurate measurements were obtained was ~ 6 kHz. Consequently, the LDV technique could not be used to obtain measurements for phase-locked analysis. Therefore, this technique was employed only to obtain circumferentially averaged time mean radial velocity and to detect flow reversal near the walls. A 5-MHz frequency shift was introduced to one of the split beams to enable the measurement of negative radial velocities and to minimize fringe bias. The LDA signal was first converted to an analog signal using a D/A converter and subsequently digitized at a constant rate of 200 samples/s. This eliminated the velocity bias and thus the need for transit time weighting. Record lengths of 90 s were used to calculate the mean velocity.

Finally, wall static pressures were measured along a radial line on both the shroud and the hub using a variable-capacitance type of pressure transducer. These measurements will partly compensate for the lack of information on the axial velocity, which is most difficult to measure using hot wires because of its small magnitude compared to V_r and V_θ . The use of LDV to measure V_z also proved impossible because of the large size of the diffuser and its small width. Consequently, it was not possible to measure V_z anywhere.

Data Acquisition and Analysis Techniques

The flow leaving the impeller is nonstationary and nonuniform both circumferentially and axially. However, if the flow is observed by a hot-wire probe placed at a fixed circumferential position at the diffuser inlet, it will appear to be periodic. The periodicity of such a signal represents the circumferential distribution of velocity at any frozen time frame. Therefore, information on the variation of the flow in both time and the circumferential coordinate can be captured by a high-frequency response probe placed at a fixed circumferential location. A short segment of such a time record is shown in Fig. 2. These are the oscilloscope traces of the uncalibrated signals;

the top trace is from the single sensor placed at the diffuser inlet, and the bottom traces are from the two sensors of the cross wire placed at a fixed radial position inside the diffuser. Both hot-wire probes were placed at an axial coordinate of $z/b=0.36$. The radial location of the cross-wire probe is $\bar{r}=0.24$. All three signals show strong periodicity. The single wire was placed normal to the radial direction and senses the radial component of velocity. The sensors of the cross wire were at ± 45 deg to the radial coordinate in a plane parallel to the diffuser walls and thus contain information on both the radial and circumferential components of velocity.

The flow configuration and the line of measurement of the cross wire are depicted in Fig. 3. Graphically shown is a set of mean streamlines, each pair of which defines a period for the cycle of flow. In the present experiment, one period equals $2\pi/17$. Each period, therefore, contains velocity information that repeats itself around the periphery of the diffuser. This cyclic behavior is captured by the cross wire, as a period in the time series record, when the flow goes past the probe, which is fixed at a radial location. From the time records at various radial locations, the periodic behavior of the flow at a given height in the diffuser is obtained. Repeating this process at dif-

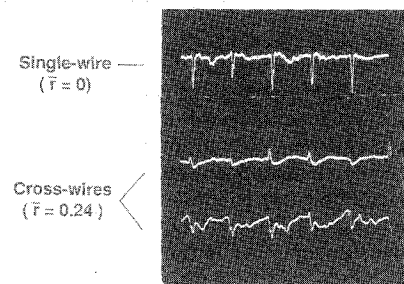


Fig. 2 Oscilloscope traces of reference-wire and cross-wire signals.

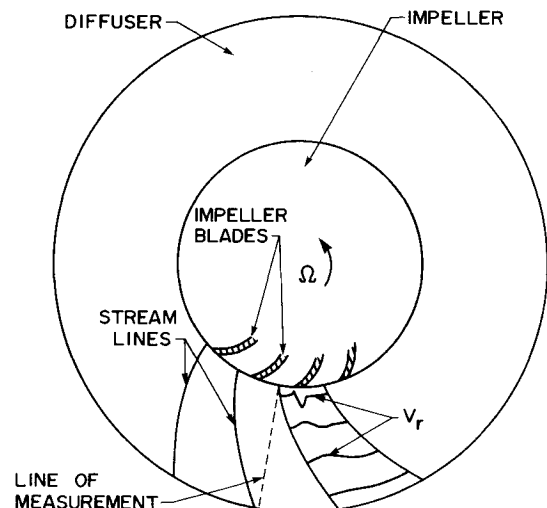


Fig. 3 Pictorial of periodic flow in diffuser.

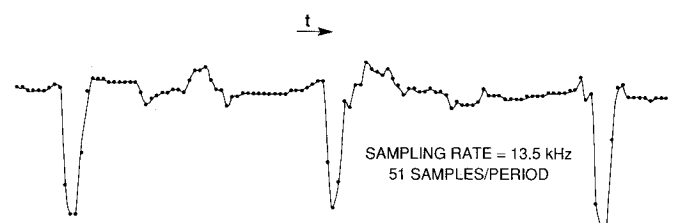


Fig. 4 A digitized trace of the single-wire signal.

ferent z/b locations, various stream segments (parallel to the diffuser walls) of periodic flow are realized. The measurements are made along a single radial line. Hence, the periods obtained at different radial locations are out of phase with one another. This is corrected with the help of the reference signal. Since the phase angle between the reference signal and the radial velocity record obtained at each location is known, the phase angle between each of these data records is easily determined.

The signals from the cross-wire probe were sampled and recorded simultaneously with the output of the single wire. The periodic behavior of the flowfield is dictated by the passage frequency of the impeller channels. In order to resolve this periodic behavior accurately, it was necessary to sample the hot-wire signals at a frequency of 9.95 kHz. At the impeller rotational speed of $\Omega = 924$ rpm, the selected conversion rate allowed 38 data points to be collected over one period. If a lower sampling rate was used, the measurements would not be able to resolve the wake behind the blades. A total record length of 6 s was used to analyze the flow at each measuring location.

The basis for the ensemble-averaging was the highly periodic reference radial velocity signal. It was used to establish the phase of the flow within the diffuser. Therefore, the beginning of each period (or cycle) in a time record, obtained from the cross-wire probe, was determined by a certain preset phase angle of the reference signal. In this way, the suspected periodic behavior of the velocities in the diffuser would be in phase with the reference signal and, thus, the phase angle between the velocities obtained at different locations could be determined. When the reference signal is nearly sinusoidal, as it is, for example, in a von Kármán vortex street, it is most convenient to choose the zero crossing (with a prescribed slope sign) of the bias-removed signal as the lock-in phase. In the present experiment, however, the periodic radial velocity at the diffuser inlet, although quite repeatable, did not exhibit a sinusoidal behavior (Fig. 4). Note that a higher sampling rate of 13.35 kHz is chosen in this preliminary measurement. Instead, the trace had a sharp dip attached to a wide but fairly uniform section. Thus, the absolute minima of the trace could be used to determine the lock-in phase of the signal. Once the starting phase angle was determined, ensemble-averaging could be carried out. This was achieved by averaging over individual time realizations that belonged only to the same phase angle. Consequently, each statistical property of the velocity components, for any given flow location, although time-averaged, was resolved over a period. A similar technique has been used to measure the flow properties in a propeller wake.⁶ Those results give revealing insight into the unsteady wake flow. Consequently, the method used in Ref. 6 to resolve the stationary statistics was also used in the present study to evaluate V_r , V_θ , v_r' , v_θ' , and the mean flow angle α . Extensive software has been developed and tested for use in data acquisition

and analysis. The flow properties thus measured are presented and analyzed in detail in the next section.

Discussion of Results

Pressure Measurements and Recirculation Ring

The wall static pressure measurements are shown in Fig. 5. Here, the normalized pressure difference $2\Delta P/\rho U_{TIP}^2$ is plotted vs \bar{r} . It was not possible to measure ΔP on the shroud side in the region $\bar{r} < 0.55$ because of the way the test model was fabricated. Therefore, the dashed line in Fig. 5 represents an educated guess on the behavior of the shroud-side ΔP . The educated guess was based on the pressure behavior within a recirculation region of a sudden-expansion flow. As expected, the flow is subject to a large adverse radial pressure gradient, and there is a significant pressure difference between the shroud and the hub at the inlet. This difference slowly disappears as the diffuser exit is approached and the hub pressure reaches a minimum at about $\bar{r} \approx 0.4$. The relatively large wall static pressure on the hub side is caused by the impeller flow, which actually enters the diffuser at an angle to the surface of the diffuser hub. Thus, this impingement of the inlet flow is responsible for the pressure difference between the shroud and the hub. As the flow accelerates in the radial direction, the hub-side static pressure drops, and a minimum is reached at about $\bar{r} \approx 0.4$. As will be seen later, this is also the approximate radial location at which the boundary layers on the hub and shroud merge.

The LDV was used to traverse the flow across the diffuser in the radial direction near the hub and the shroud to detect reversed flow. At a mass flow rate of 0.162 kg/s and an $\Omega = 924$ rpm, no flow reversal was detected on the hub side. However, a large flow reversal region was measured on the shroud side. In order to assess whether this flow reversal led to stalled flow behavior in the diffuser, dynamic pressure measurements were carried out to determine the existence of rotating stall cells, using the technique described in Ref. 7. No periodic behavior of the pressure was observed to indicate rotating stall. The LDV was then moved to another circumferential position to traverse the flow near the shroud from $\bar{r} = 0$ to $\bar{r} = 1.0$. Again, a recirculation region of about the same size as before was measured. This showed that the recirculation region has the shape of a ring, whose size is indicated as the locus of $V_r = 0$ in Fig. 6. Right at the inlet, the flow is forward across z up to $z/b \approx 0.8$ and essentially zero in the region $0.8 < z/b \leq 1$. The recirculation ring extends from $\bar{r} = 0$ to $\bar{r} \approx 0.87$ in the radial direction and to $z/b \approx 0.65$ in the axial direction at its maximum.

This flow characteristic resembles very much that of the flow through an axisymmetric sudden expansion.¹⁰⁻¹² In the present study, the gap between the casing and the top of the impeller, which acts as a sudden-expansion step, is $0.25b$, and the estimated reattachment length is about 12 step heights (Fig. 6), which is consistent with other measurements.¹⁰ However, there are three major differences between this flow and

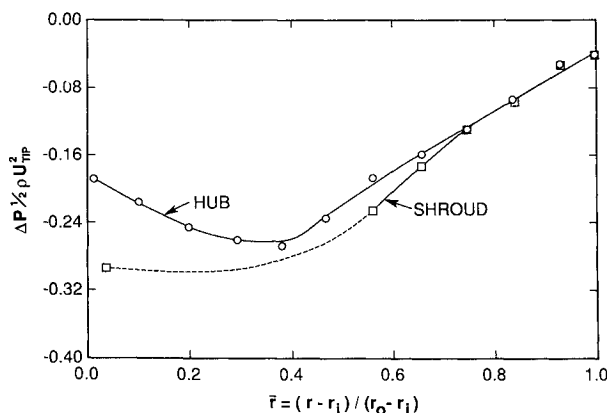


Fig. 5 Pressure difference measurement between shroud and hub.

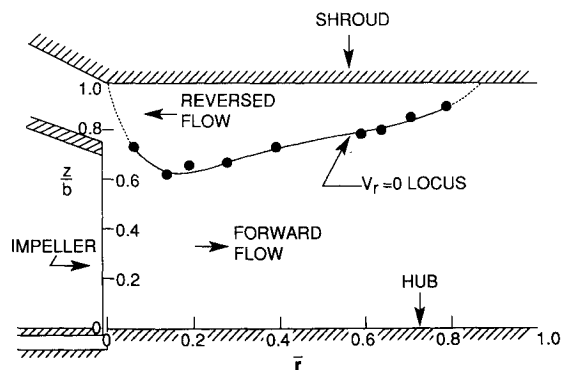


Fig. 6 The recirculation ring on the shroud side.

the other sudden-expansion flows,^{10,11} including those with axial rotation.¹² First, flow rotation is about an axis normal to the flow direction. Second, there is a nonzero axial velocity V_z at the inlet, which is absent in all sudden-expansion flows examined in the past.^{10,11} Third, in the present flow, there is a gap in place of a vertical wall. These could be the reasons why the mean separation streamline originates from the shroud rather than from the impeller top edge and extends to below the top of the impeller. The dashed line shown near the inlet implies that locally separated flow could exist on the shroud side of a vaneless diffuser without triggering the onset of rotating stall. The LDV data shown in Fig. 6 are also consistent with the ΔP distribution (Fig. 5) and point to the presence of a significant V_z component in the inlet region of the vaneless diffuser.

Circumferentially Averaged Flow Behavior

In view of the existence of the recirculation ring and the inability of the current LDV setup to give a high enough data rate, the hot-wire measurements were limited to the region $0 < z/b \leq 0.6$. The reason for this limited axial traverse is the inability of the hot wire to resolve flow direction. Consequently, it was not used to measure the flow inside the recirculation ring. Altogether, five cross-wire measurements were carried out at $z/b = 0.12, 0.24, 0.36, 0.48$, and 0.6 for each \bar{r} location, and a total of six \bar{r} locations were investigated. These were chosen at $\bar{r} = 0.0, 0.21, 0.41, 0.61, 0.81$, and 1.0 , so that a full set of inlet profiles is available for model calculations. The LDV was also used to measure the circumferentially averaged mean V_r in the region $0.6 < z/b < 1$ for each selected \bar{r} location. These measurements, together with the cross-wire results, are used to construct a set of V_r , V_θ , and α profiles across z at each of the \bar{r} locations investigated. The circumferentially averaged V_r , V_θ , and α are shown in Fig. 7. The inlet flow is very uniform across z in the region $0.1 < z/b < 0.5$, and V_r , V_θ , and α are essentially constant. The flow angle at the diffuser inlet is about 64 deg, which is far

below the critical flow angle of ~ 78 deg for the onset of rotating stall.^{3,13,14} This again confirms that the present flow is free of rotating stall cells, in spite of the existence of the recirculation ring on the shroud side.

Figure 7 shows that intense axial mixing is present in the region $0 < \bar{r} < 0.4$. This is indicated by the quick disappearance of the constant behavior of V_r and V_θ across z at $\bar{r} = 0.21$ and means that the initial hub-side boundary layer has rapidly grown to mix with the external flow. By $\bar{r} = 0.41$, the two wall boundary layers have completely merged, thus, implying that boundary-layer type of analyses are inappropriate for vaneless diffuser flows and that a full three-dimensional approach has to be used to analyze such flows. Beyond $\bar{r} = 0.41$, V_θ and α slowly recover their uniform behavior across z and at the exit. The mean flow angle is averaged about 68 deg, whereas V_θ is about 2.7 m/s and represents a decrease of approximately 40% from the diffuser inlet. Finally, it should be pointed out that the velocity measurements satisfy mass conservation, as demonstrated by a simple calculation using the measured profiles.

Flow Variations over One Period

Even though measurements at six \bar{r} locations are available, only those at $\bar{r} = 0.0, 0.21$, and 0.81 are shown in Figs. 8–13. The reason is that the measurements at $\bar{r} = 0.41, 0.61, 0.81$, and 1.0 are very similar in their general behavior, which is reflected in the circumferentially averaged properties shown in Fig. 7. The flow properties over one period are plotted vs the dimensionless period $17\theta/2\pi$, and the mean quantities are

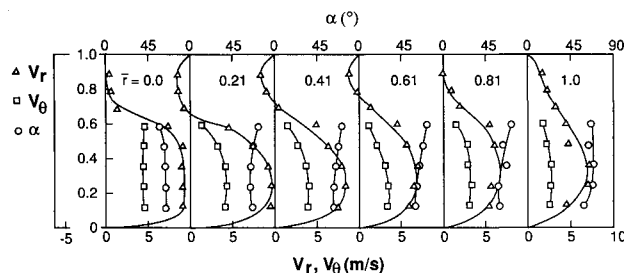


Fig. 7 Circumferentially averaged profiles of V_r , V_θ , and α at different \bar{r} locations.

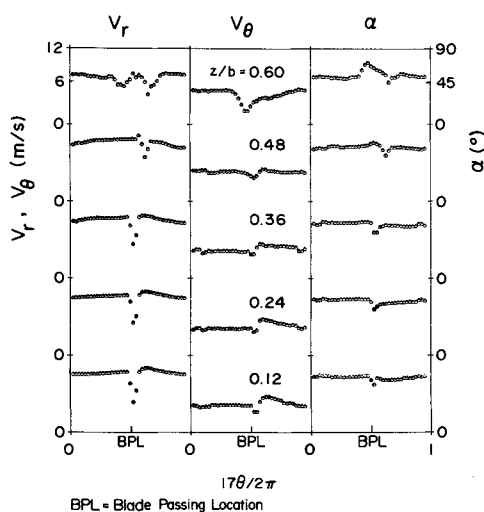


Fig. 8 Periodic behavior of mean velocities and flow angle at $\bar{r} = 0$.

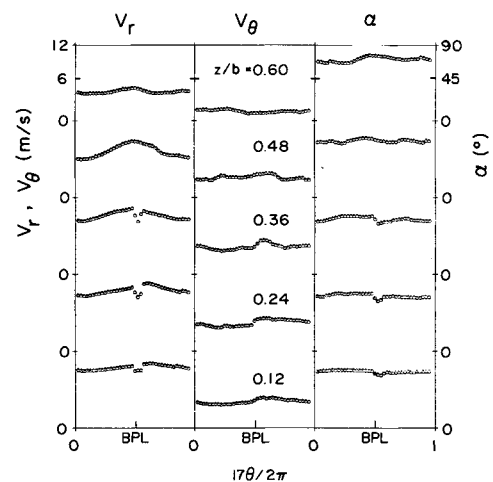


Fig. 9 Periodic behavior of mean velocities and flow angle at $\bar{r} = 0.21$.

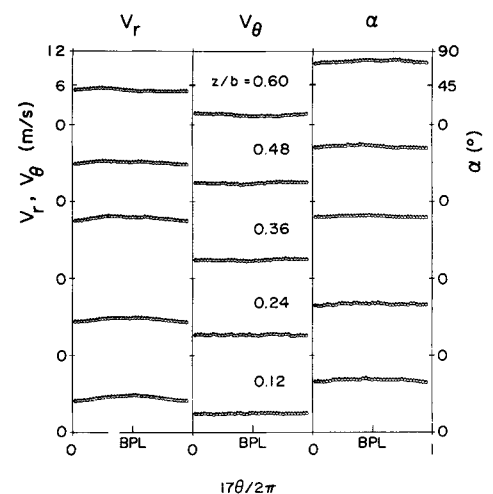


Fig. 10 Periodic behavior of mean velocities and flow angle at $\bar{r} = 0.81$.

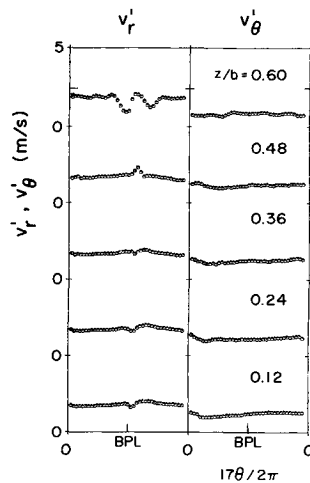


Fig. 11 Periodic behavior of turbulent properties at $\bar{r}=0$.

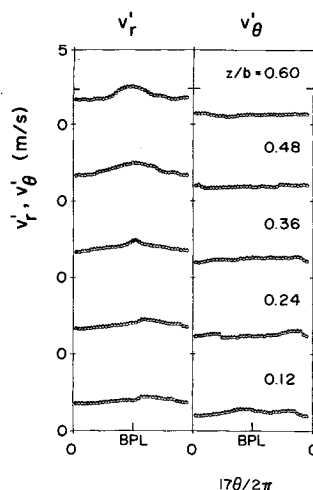


Fig. 12 Periodic behavior of turbulent properties at $\bar{r}=0.21$.

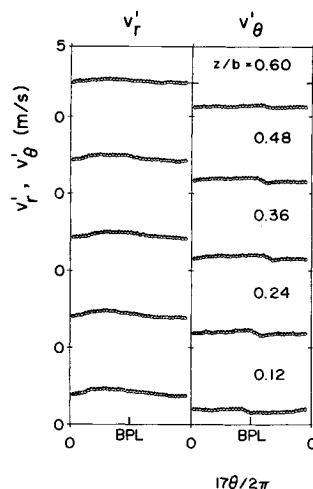


Fig. 13 Periodic behavior of turbulent properties at $\bar{r}=0.81$.

shown in Figs. 8–10, whereas the turbulence properties are given in Figs. 11–13.

The jet/wake behavior of the flow over one period at the diffuser inlet is clearly indicated in Fig. 8. The flow is uniform over one period except in the region where the wake is present. The radial velocity slightly overshoots on the trailing side of the impeller blade, which is a consequence of flow rotation and the high degree of camber in the impeller channels. The

wake region is very narrow and amounts to about 0.1 of the width of the impeller blade passage. Furthermore, the wake width remains rather uniform across z in the region $0 < z/b < 0.5$. At $z/b = 0.6$, the wake spreads wider, and a second dip is noticed in V_r . It is not known what causes this second dip. However, the interaction of the forward flow with the separated flow in the recirculation ring and the effects of sudden enlargement could be partially responsible for the second dip. Nevertheless, the second dip disappears as the flow moves to $\bar{r} = 0.21$ (Fig. 9). The jet/wake behavior is also clearly visible in the θ variation of V_θ and α . Their profiles follow closely that of V_r (Figs. 8 and 9).

The periodic behavior remains with the flow all through the diffuser in both the r and z directions although it becomes much weaker near the diffuser exit (Figs. 8–10). This is evident from the results obtained through the phase-locked ensemble-averaging technique and the fact that the values of V_r , V_θ , and α at the beginning of a period are the same as those at the end of the same period. However, the wake signature disappears slowly inside the diffuser. By $\bar{r} = 0.41$, the wake signature is not noticed anywhere in the flow, and V_r is nearly uniform except for the weak periodicity. The uniformity persists all the way to the exit of the diffuser. A representative plot of this behavior is shown in Fig. 10.

The behavior of the turbulent normal stresses, shown in the form of v_r' and v_θ' in Figs. 11–13, follows closely the development of V_r and V_θ . Again, at $\bar{r} = 0$ and $z/b = 0.60$, two dips are observed in the distribution of v_r' over one period, and it, too, disappears at $\bar{r} = 0.21$. The magnitudes of v_r' and v_θ' indicate a high level of turbulence activity and thus intense mixing inside the diffuser ($v_r'/V_r \approx 0.22$ and $v_\theta'/V_\theta \approx 0.26$). In view of their large magnitude, the accuracy of the turbulence measurements will not be as good as that for the mean flow quantities. In general, v_r' is larger than v_θ' everywhere in the diffuser and is fairly constant across z . Thus, the turbulence field is anisotropic, and the normal stress component in the radial direction is larger than that in the circumferential direction. Therefore, for a given operating condition, the diffuser flow in the radial direction has a greater amount of total kinetic energy available to overcome separation that may be caused by the radial adverse pressure gradient.

Another point to note about v_r' and v_θ' is their values at the beginning and end of each period. The fact that they are equal shows that the turbulence field is also periodic; hence, the turbulence field within one period is stationary. This essentially verifies the technique used to acquire and analyze the flow properties. Therefore, in spite of the fact that, in general, the diffuser flow is unsteady and nonstationary, within one period it is steady and stationary and can be resolved by the phase-locked technique.

Conclusions

A phase-locked ensemble-averaging technique has been developed to resolve the unsteady and nonstationary turbulent flow in a vaneless diffuser. The technique depends on the use of a reference hot wire placed at the diffuser inlet and circumferentially displaced from the measurement locations to pick up the reference phase for the analysis of the cross-wire signals. It is found that the stall-free flow inside the vaneless diffuser is periodic, in spite of the existence of a recirculation ring on the shroud side. Within one period, the flow is steady and stationary. Therefore, the averaging technique gives the true behavior of the flow within one period. The flow properties measured were the wall static pressure and the mean and fluctuating radial and circumferential velocities.

The gap between the casing and the top of the impeller gives rise to a sudden expansion of the impeller flow into the diffuser. This, in turn, creates a recirculation ring on the diffuser shroud. The presence of the recirculation ring does not lead to a stalled flow because the diffuser inlet flow angle is substantially lower than the critical angle for the onset of rotating stall. This means that locally separated flow can exist on the

shroud side even in a flow free of rotating stall. The pressure measurements indicate that the flow delivered from the impeller is not parallel to the hub surface. Instead, the flow emerging from the impeller impinges on the hub surface at an angle and thus enhances flow mixing in the axial direction. A consequence of this is the rapid merging of the wall boundary layers. This means that boundary-layer-type analyses of vaneless diffuser flows are not appropriate. Also, the downward axial velocity tends to increase the axial extent of the recirculation ring.

The results further show that the flow at the inlet of the diffuser displays a jet/wake type of flow behavior within one period. Outside the wake, V_r and V_θ are quite uniform. The wake is rather narrow and occupies about 0.1 of the width of an impeller channel. However, the wake signature disappears beyond $\bar{r}=0.21$, a consequence of the enhanced circumferential mixing due to flow rotation. As the flow expands through the diffuser, V_r increases near the shroud but decreases near the hub, whereas, V_θ remains fairly constant across z . The turbulence field behavior essentially follows the same trend, but the turbulence intensities measured within one period are anisotropic, with v_r' significantly greater than v_θ' . Furthermore, the radial decay of the circumferentially asymmetric character of the flow is relatively slow and, although weak, the periodic behavior is still detectable, even near the diffuser exit.

Finally, the present measurements contribute data that can enhance the development of a numerical model for the calculation of unstalled flow in vaneless diffusers.

Acknowledgment

Funding support from the Naval Ship Research and Development Center, Annapolis, Maryland, under Contract N00167-86-K-0075, is gratefully acknowledged.

References

¹Dean, R. C., and Senoo, Y., "Rotating Wakes in Vaneless Diffusers," *Journal of Basic Engineering*, Vol. 88, Jan. 1960, pp. 49-60.

²Eckardt, D., "Instantaneous Measurements in the Jet-Wake Discharge Flow of a Centrifugal Compressor Impeller," *Journal of Engineering for Power*, Vol. 97, 1975, pp. 337-346.

³Ligrani, P. M., Van Den Braembussche, R., and Roustan, M., "Measurements in the Vaneless Diffuser of a Radial Flow Compressor," *International Journal of Heat and Fluid Flow*, Vol. 4, 1983, pp. 103-106.

⁴Krain, H., "A Study on Centrifugal Impeller and Diffuser Flow," *Journal of Engineering for Power*, Vol. 103, 1981, pp. 688-697.

⁵Senoo, Y., and Ishida, M., "Behavior of Severely Asymmetric Flow in a Vaneless Diffuser," *Journal of Engineering for Power*, Vol. 97, 1975, pp. 375-387.

⁶Cenedese, A., Accardo, L., and Milone, R., "Phase Sampling in the Analysis of a Propeller Wake," *Journal of Engineering for Power*, Vol. 97, 1988, pp. 55-60.

⁷Otugen, M. V., So, R. M. C., and Hwang, B. C., "Diffuser Stall and Rotating Zones of Separated Boundary Layer," *Experiments in Fluids*, Vol. 6, 1988, pp. 521-533.

⁸Senoo, Y., Kinoshita, Y., and Ishida, M., "Asymmetric Flow in Vaneless Diffusers of Centrifugal Blowers," *Journal of Fluids Engineering*, Vol. 99, 1977, pp. 104-114.

⁹So, R. M. C., Ahmed, S. A., and Mongia, H. C., "Jet Characteristics in Confined Swirling Flows," *Experiments in Fluids*, Vol. 3, 1985, pp. 220-230.

¹⁰So, R. M. C., "Inlet Centreline Turbulence Effects on Reattachment Length in Axisymmetric Sudden-Expansion Flows," *Experiments in Fluids*, Vol. 5, 1987, pp. 424-426.

¹¹So, R. M. C., and Ahmed, S. A., "Characteristics of Dump Combustor Flows," *International Journal of Heat and Fluid Flow*, Vol. 10, 1989, pp. 66-74.

¹²So, R. M. C., and Ahmed, S. A., "Rotation Effects on Axisymmetric Sudden-Expansion Flows," *Journal of Propulsion and Power*, Vol. 4, July-Aug. 1988, pp. 270-276.

¹³Van Den Braembussche, R., Frigne, P., and Roustan, M., "Rotating Non-uniform Flow in Radial Compressors," AGARD CP-282, Paper 12, 1980.

¹⁴Kinoshita, Y., and Senoo, Y., "Rotating Stall Induced in Vaneless Diffusers of Very Low Specific Speed Centrifugal Blowers," *Journal of Engineering for Gas Turbine and Power*, Vol. 107, 1985, pp. 514-521.

Recommended Reading from the AIAA Progress in Astronautics and Aeronautics Series . . .



Gun Propulsion Technology

Ludwig Stiefel, editor

Ancillary to the science of the interior ballistics of guns is a technology which is critical to the development of effective gun systems. This volume presents, for the first time, a systematic, comprehensive and up-to-date treatment of this critical technology closely associated with the launching of projectiles from guns but not commonly included in treatments of gun interior ballistics. The book is organized into broad subject areas such as ignition systems, barrel erosion and wear, muzzle phenomena, propellant thermodynamics, and novel, unconventional gun propulsion concepts. It should prove valuable both to those entering the field and to the experienced practitioners in R&D of gun-type launchers.

TO ORDER: Write, Phone, or FAX: AIAA c/o TASC0,
9 Jay Gould Ct., P.O. Box 753, Waldorf, MD 20604
Phone (301) 645-5643, Dept. 415 ■ FAX (301) 843-0159

Sales Tax: CA residents, 7%; DC, 6%. For shipping and handling add \$4.75 for 1-4 books (call for rates for higher quantities). Orders under \$50.00 must be prepaid. Foreign orders must be prepaid. Please allow 4 weeks for delivery. Prices are subject to change without notice. Returns will be accepted within 15 days.

1988 340 pp., illus. Hardback
ISBN 0-930403-20-7
AIAA Members \$49.95
Nonmembers \$79.95
Order Number V-109